Journal of Geochemical Exploration 198 (2019) 71–81

Contents lists available at ScienceDirect

Journal of Geochemical Exploration

journal homepage: www.elsevier.com/locate/gexplo

Delineation of deep prospecting targets by combining factor and fractal analysis in the Kekeshala skarn Cu deposit, NW China

Zhonglin Xiang[a], Xuexiang Gu[b,*], Enying Wang[a], Xinli Wang[c], Yongmei Zhang[b], Yan Wang[a]

[a] Institute of Resources and Environment, Henan Polytechnic University, Jiaozuo 454000, China
[b] School of Earth Sciences and Resources, China University of Geosciences, Beijing 100083, China
[c] Xinda Gold & Silver Development Centre, Beijing 100038, China

ARTICLE INFO

Keywords:
Borehole primary halo
Factor analysis
C–V fractal model
3D geological modeling
Kekeshala skarn-Cu deposit

ABSTRACT

Three-dimensional visualization, factor analysis, and fractal/multifractal modeling are combined to study the geochemical data of borehole primary halo in the Kekeshala mining area in Northwestern China to screen exploration targets. First, based on the borehole spatial database comprising collar, survey, geology, and sample tables, 3D borehole primary halo samples are extracted. Their 3D block model is then constructed by spatial interpolation. Second, sample factor analysis of the borehole primary halo mainly includes four factors: F1 consists of Ag–Cu–Sn combination, F2 consists of Pb–Zn combination, F3 consists of As–Sb combination, and F4 consists of Mo–W combination. Moreover, 3D geochemical zoning is conducted for the samples. Third, based on the 3D block model of the primary halo, the F1 factor score is further modeled by Concentration–Volume (C–V) fractal model. Furthermore, based on the fractal fitting line's four segments obtained from the inflection points, geochemical barren host rocks, weakly deep prospect, moderately deep prospect, and highly deep prospect are extracted. Results indicate the following: (a) the F1 factor embodies the main metallogenic process or stage, which can be used as a comprehensive indicator of the spatial aggregation of major metallogenic elements in the study area; (b) the C–V fractal model can effectively determine the F1 factor deep prospect threshold of the skarn-Cu deposit in Kekeshala; and (c) the moderately and highly deep prospects of the F1 factor can well reflect the favorable geological conditions of metallogenesis and be used as the basis for delineating the prospecting target. Therefore, the fractal deep prospect of the geochemical F1 factor of the borehole primary halo has a good application effect in deep prospecting and prediction, which can be effectively used to explore the depth and edge of known deposits.

1. Introduction

The geological anomaly theory is a basic theory that guides ore prospecting (Zhao and Chi, 1991), indicating that primary geochemical halo anomalies are the most economical and effective methods for delineating mineralized zones from barren host rocks in 3D geochemical exploration. The investigation of metallogenic elements and paragenetic sequence provides useful data for ore-forming processes in deposits, because the characteristics of various types of ore deposits are reflected by their element assemblages. Factor analysis, an effective method to study the symbiotic combination of elements, can realize the division of different geochemical backgrounds (Shi et al., 2004; Zhao et al., 2012; Liu et al., 2015), can reflect the regional metallogenic geological background, and can reveal the spatial variation characteristics of the metallogenic element and its elemental combination. The analysis factor, reflecting the main metallogenic information (element combination), is more meaningful than the traditional single element or other multielement combination in abnormity assessment.

Mineralization involves huge energy release or supernormal enrichment and the accumulation of matter within a relatively short time interval or space range, especially in endogenetic hydrothermal metallogenic system. The ore source and the ore-forming fluid are often restricted by the heterogeneity of material distribution and the earth's tectonic activity and evolution. The enrichment and depletion of ore minerals and ore-forming elements are complex nonlinear processes (Cheng, 2008). In recent years, the fractal theory based on the fractal geometry proposed by Mandelbrot (1983), which is an effective nonlinear research tool, has made a series of research achievements in geochemistry (e.g. Turcotte, 1986; Agterberg et al., 1993; Cheng et al., 1994; Sim et al., 1999; Goncalves et al., 2001; Li et al., 2003; Carranza

* Corresponding author.
E-mail address: xuexiang_gu@cugb.edu.cn (X. Gu).

https://doi.org/10.1016/j.gexplo.2018.12.004
Received 1 August 2018; Received in revised form 8 November 2018; Accepted 9 December 2018
Available online 12 December 2018
0375-6742/

et al., 2009; Carranza and Sadeghi, 2012; Zuo et al., 2009a, 2009b, 2009c, 2009d; Afzal et al., 2010; Wang et al., 2011; Cheng, 2011; Zuo, 2011a, 2011b; Cheng, 2012; Zhang and Zhou, 2012; Zuo et al., 2015). Several fractal models have been developed and applied to geochemical exploration by separating various geochemical populations (including mineralized zones and phases), such as concentration–area (C–A) by Cheng et al. (1994), concentration–distance (C–D) by Li et al. (2003), concentration–volume (C–V) by Afzal et al. (2011), and number–size (N–S) by Mandelbrot (1983) and Agterberg (1995). Fractal analysis assists in describing the relationships among geological, geochemical, and metallogenic settings with the spatial information from the analysis of primary-halo geochemical data. Various geochemical processes can be explained due to the differences in fractal dimensions obtained from the analysis of relevant geochemical data. In this paper, C–V fractal model was utilized for delineating the prospecting target in the skarn copper deposit in Kekeshala, Northwestern (NW) China. The multifractal characteristics of the main metallogenic factors in factor analysis and the application effect of prospecting are discussed.

2. Methodology

Results derived from the 3D borehole, factor analysis, and fractal/multifractal modeling are combined in delineation of potential targets in the skarn copper deposit in Kekeshala, NW China. The 3D borehole database of the Kekeshala deposit was constructed using 167 boreholes and 4878 samples from the borehole dataset. The factor analysis involved information from the synthesis of 11 trace elements in the primary halo of the borehole and the extraction of main ore-forming or ore-indicating factors. The fractal models used include (a) the estimation of ore-forming or ore-indicating factors in the analysis of primary halo factor from the borehole dataset to model the continuity of mineralization and (b) the application of the C–V fractal model to define a threshold value for the ore element to constrain the mineralization fluid center or a path in a 3D block model (Afzal et al., 2011; Sadeghi et al., 2012; Ebadi Rajoli et al., 2015; Afzal et al., 2015). This study aims to identify potential copper targets through the methods mentioned.

2.1. 3D borehole database

Deep geochemical exploration and geological data are generally obtained through engineering drilling (e.g., in addition, pit exploration, trough exploration, etc.). Information on spatial location and basic lithology and the sample analysis data are obtained by drilling holes. Considering the redundancy and reference integrity of the data, we use the relational database model to divide the borehole information into 4 basic correlation tables: collar, survey, geology, and sample tables (Table 1). Each table is related by the “Hole_ID”.

By using digital mine software such as Surpac, the data from the above tables are imported to establish the borehole geological information database and display the geological engineering data in 3D space, including the borehole trajectory line, lithology and character description, grade value, sampling trajectory. Subsequently, the geological phenomena are analyzed in 3D space. The 3D discrete sample data are extracted using the data extraction function module of the borehole database. Information on the central position (including sample length) and the analysis data corresponding to the trace elements of the sample are stored in the form of 3D points. During spatial interpolation, it is generally necessary to analyze the variation of sample length and element value for a more objective sample location information and to generate sample data with uniform sample length.

Table 1
Field information in the borehole database.

Table name	Field
Collar	Hole_ID, Y, X, Z, Max_depth, Hole_path
Survey	Hole_ID, Depth, Azimuth, Dip
Geology	Hole_ID, Samp_ID, Depth_from, Depth_to, Rock_type
Sample	Hole_ID, Samp_ID, Depth_from, Depth_to, Cu, Au, etc.

2.2. Factor analysis

Factor analysis can be used to determine the symbiotic association of elements with diagenesis and metallogenesis, and the use of factor score map can reveal the relationship between assemblage anomalies and geological bodies (e.g., strata, intrusive rocks, orebodies) in space (Davis, 1973; Zhang, 1989; Agnew, 2004). The steps in factor analysis include determining factor load, carrying out factor rotation, and calculating the factor score, where the initial factor load matrix is not unique, and the meaning of the factor is often ambiguous. Hence, the initial load matrix needs to be rotated to obtain a more practical public factor. In this paper, based on the borehole primary halo, the factor analysis is done by using the SPSS software. Moreover, the main factors whose eigenvalue is greater than 1 are obtained, and the elemental combination and factor score are determined.

2.3. Fractal modeling

Since the 1980s, fractal and multifractal models have been effectively used to describe the distributions of geological objects, especially mineralization features (Agterberg, 2012; Bansal et al., 2011; Carlson, 1991; Carranza et al., 2009; Cheng, 1995, 2004; Cheng et al., 1994; Mandelbrot, 1983; Raines, 2008; Turcotte, 1997; Zuo et al., 2009a, 2009b, 2009c, 2009d; Zuo, 2011a, 2011b, 2012; Zuo et al., 2013; Sadeghi et al., 2012; Ebadi Rajoli et al., 2015; Afzal et al., 2015). Fractal analysis can be used to indicate and justify the differences among the mineralization, alteration, lithology, and zonation of ore deposits especially in hydrothermal occurrences (Cheng, 2007; Carranza, 2008; Carranza et al., 2009; Afzal et al., 2011, 2012; Wang et al., 2011a, 2011b, 2012). Afzal et al. (2011) proposed the C–V fractal model for delineating supergene enrichment and hypogene zones from oxidation zones and the barren host rocks in porphyry-Cu deposits. The C–V fractal model can be expressed as follows:

$$V(\rho \le \upsilon) \propto \rho^{-a}{}_1;\ V(\rho \ge \upsilon) \propto \rho^{-a}{}_2 \quad (1)$$

where $V(\rho \le \upsilon)$ and $V(\rho \ge \upsilon)$ denote two volumes with concentration values (ρ) less than or equal to and greater than or equal to, respectively; υ represents the threshold value of a mineralized zone (or volume), and a_1 and a_2 are characteristic exponents.

The log–log plots of the corresponding volumes $V(\rho \le \upsilon)$ and $V(\rho \ge \nu)$ follow a power-law relationship, where the linear relationship of V varies at different ρ intervals, as indicated by several straight lines. This linear relationship can be fitted using the least square method. These different linear segments reflect different fractals between $V(\rho \ge \upsilon)$ and ρ and may also represent the difference in metallization or stages of major metallogenic processes (Afzal et al., 2016; Hashemi Marand et al., 2018).

In this paper, the C–V fractal model was utilized for delineating and classifying synthetic deep prospects exposed by main metallogenic factor on primary halo in borehole to delineate various enriched zones and rocks in the skarn copper deposit. The terms “highly deep prospect”, “moderately deep prospect”, “weakly deep prospect”, and “barren host rocks” are used to classify the mineralized zones in the deposit based on C–V fractal modeling in 3D space. The main distribution block models of the metallogenic factor for the study area were generated using the ordinary inverse distance weighted (IDW) interpolation method using the Surpac software. The volume or percentage of blocks with different scores is obtained statistically. The C–V fractal method can be implemented using the Excel software. First, a text file for the statistical data of the 3D interpolation block model is imported and read. Then, the scores of the main metallogenic factor are

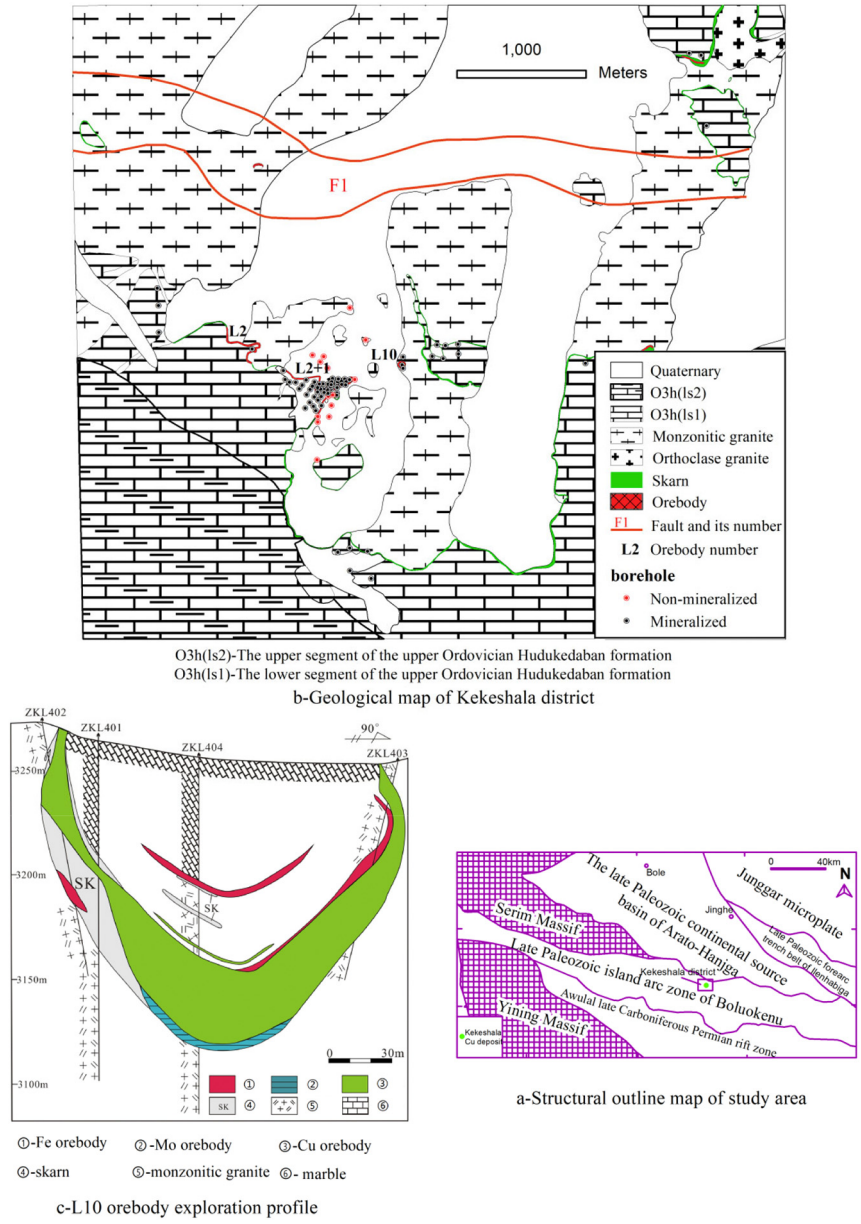

Fig. 1. Geological map of the Kekeshala copper deposit and the exploration profile of the L10 ore body.

sorted form high to low. Afterwards, the number of voxels for each factor score interval are counted, their accumulated value in the deposit district is computed. Finally, the logarithm of all data for metallogenic factor scores and the accumulated frequency values are calculated before drawing the C–V log–log plot.

3. Geological setting and datasets

The Kekeshala copper district (ca. 28 km^2) is situated in the Boluokenu metallogenic belt in NW China. It can be divided into three ore sections: Kekeshala, Aimusidaiyi, and Xiangtou shan. The 3D study area is situated within the coordinates 4,883,360–4,888,284 N and 636,106–641,630 E. The elevations, including the subsurface portions of the model, range from 2500 m to −3850 m relative to the sea level (Figs. 1 and 2).

The copper district is located in the Boluokenu island arc, which went through the Proterozoic ancient craton formation, the Sinian–Cambrian stable sedimentation, the Ordovician–Silurian ancient craton disintegration, the Silurian–Carboniferous extensional aggregation alternate stage, Carboniferous–Permian intracontinental extensional rift, and the late Permian intracontinental orogeny and Foreland basin formation. Sedimentary caprocks represented by the Paleozoic are formed, accompanied by large-scale granite intrusive activities and multiple changes in regional fault structures, which create good material sources and thermodynamic conditions for mineralization in this area. The outcrop formation is relatively simple, including only the upper Ordovician Hudukedaban formation (O_3h) and Quaternary (Q). The Hudukedaban formation involves a set of shallow marine carbonate rocks, which generally shows the NW–SE extension anticline. Its Southwest Wing yields 210°–230°∠ 56°–78°, while its Northeast wing produces 50°–110°∠ 56°–60°. According to its lithological characteristics, the formation can be divided the upper and lower sections. The lower section (ls1) consists of a gray-black thin layer of bright grain limestone (local calcareous siltstone intercalation), which is mainly distributed in the south, middle (occurring as a limestone trap), and northeast corner of the mining area. The upper segment (ls2) consists of a grayish-white thick-layered, massive microcrystalline limestone, which is mainly distributed in the southwest and southeast

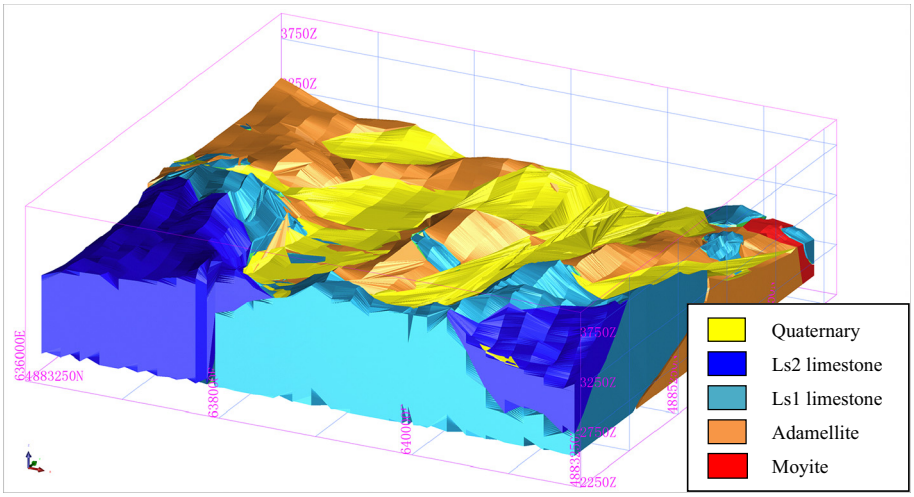

Fig. 2. 3D geological model of the Kekeshala district.

corners of the mining area. Quaternary (Q) is mainly composed of alluvial, slope, and moraine, which are distributed in the hillsides and gullies of the mining area. The outcropping structure of the mining area is simple. In the northern rock mass, a positive fault fracture zone (F1) occurs, with a broken bandwidth of 200–400 m. Its overall trend is NEE, and the fault occurred at 5°–20°∠62°–65°, which has no influence on the ore body in the mining area. The magmatic rocks in the copper district mainly include intrusive rocks, particularly biotite monzogranites, which are distributed in most areas under study. The magma intrusions are generally basic-like (i.e., the southeastern margin of the Huster rock mass) with a large scale, and the long axis is nearing the northwest direction, which is in line with the regional tectonic line. The LA–ICP–MS zircon U–Pb age of the diagenetic rocks is (368.0 ± 3.6) Ma (Gu et al., 2013), which indicates that the Huster intrusive body formed in the tectonic setting of the North Tianshan Ocean subduction southward from the Devonian to the early late Carboniferous. The intrusive rock mass was intruded into the Hudukedaban formation with a zigzag contact surface. The contact metamorphism of skarn, silicification, marble, and others occurred within the contact zone. The rock mass was in passive emplacement, and the contact surface was extroverted.

The Kekeshala copper deposit, a typical skarn deposit that occurs in the inner skarn of the late Devonian acid intrusive body and the Ordovician Hudukedaban formation limestone, which is formed through the hydrothermal metasomatism of ore-bearing hydrothermal fluids. The orebody is veined, lenticular, and cystic, and its dip angle is 50°–80°, which is strictly controlled by skarn belts and is in abrupt contact with the surrounding rocks. The main ore bodies include L2, L2 + 1, and L10. The ore body mainly consists of copper, with a few of iron, lead, zinc, and other metallic elements. The main ore type in the ore deposit is sulfide ore (chalcopyrite), while the main metal minerals include chalcopyrite and a few porphyry copper ore and molybdenite. The wall rocks near the ore body mainly consist of monzonite, granodiorite, garnet skarn, and marble. According to the mineral symbiotic assemblage and the intercalation relationship between different minerals, the metallogenic stages of the deposit are divided into skarn, quartz–sulfide, and supergene phases. The copper sulfide ore (chalcopyrite) is formed in the early sulfide stage of the quartz–sulfide period. The ore-forming controlling factor is the contact zone structure. The skarn contact zone is the most direct prospecting indicator.

Basic datasets from the copper deposit in Kekeshala include the 1:2000 scale geological map, 1:2000 scale topographic maps, and 4878 assay samples from 167 boreholes (Fig. 3), which were provided by the Seventh Geological Group of Xinjiang Geology and Mining Bureau, 2016. The dimensions of the borehole spacing vary from 40 m × 20 m to 130 m × 80 m according to the standard for copper deposit exploration in China. Among the 167 boreholes, 153 intersected mineralized rocks, while the other 14 boreholes intersected non-mineralized rocks only. Among the 167 boreholes, 87 were sunk into the orebody L2 + 1 for the evaluation of the skarn copper deposit in Kekeshala, 9 boreholes were sunk into orebody L10, 400 m to the east, and the other boreholes are scattered and distributed in several other mineralized areas to explore for the undiscovered skarn copper deposit(s).

4. Results and discussion

4.1. Dataset of borehole primary halo and closure effect analysis

The borehole samples were crushed, reduced in volume, and pulverized to 200 mesh. Geochemical analyses of samples were performed using different methods at the Seventh Geological Group Analytical Laboratories of Xinjiang Geology and Mining Bureau in China. Au was dissolved in aqua regia and fluoride and then enriched using activated carbon, while Ag was dissolved in aqua regia. Both concentrations were determined through flame atomic absorption spectrometry. Ba was melted using $NaCO_3$, while Cu, Mo, Pb, W, Sn, and Zn were dissolved by the mixture of hydrochloric acid, nitric acid, hydrofluoric acid, and perchloric acid. The results were determined by ICP–OES and full-spectrum direct-reading plasma-emission spectrometry. As, Sb, and Bi were dissolved in aqua regia, and their concentration was determined through atomic fluorescence spectrometry. A total of 4878 samples were collected from different depths of the borehole in the district. The statistical characteristics of each element are shown in Table 2.

The geochemical data generally consist of the typical composition data, and their “closure effect” have been widely known (Aitchison, 1984). In the closure effect, the total amount of all components (element contents) is constant (e.g., equal to 1 or 100%), the components are mutually restricted, and a certain pseudocorrelation exists between the components. For example, the main components, SiO_2 and Al_2O_3, are often negatively correlated with the petrochemical analysis data. Geochemists believe that the data should be “turned on” before mathematical processing. At present, the most popular method is log ratio transformation, such as additive (alr), centered (clr), and isometric-logarithmic ratio transformation (ilr) (Egozcue et al., 2003).

However, these transformations are not very suitable for the statistical analysis of R-type geochemical data involving only trace elements. For example, the data transformed by the clr are collinear and are not suitable for robust covariance estimation (Filzmoser et al., 2009). Moreover, the assumption of factor analysis is not satisfied, because the KMO and Bartlett sphericity test are not passed. For the ilr

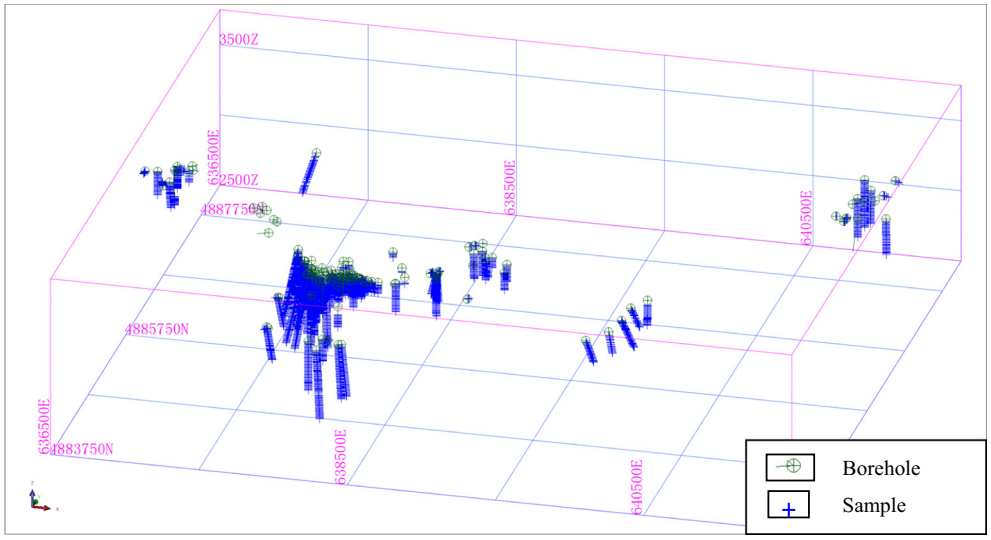

Fig. 3. 3D borehole and sample distribution of the Kekeshala district.

and alr defects, the transformed vector is one component less than the original one, while ilr assumes that the sum of components is 1. However, it is not guaranteed by trace elements, because the trace element contents in geological samples are very small with a difference of almost four orders of magnitude from the major elements. Hence, it is weakly affected by the overall closure effect. In addition, the relationship between ilr variable and the original data is related by the nonlinear function, and the linear correspondence between ilr and original variable is lost, making it difficult to make a direct geological interpretation (Egozcue et al., 2003).

In substance, the correlation between trace elements is related to the capacity (total content) of all elements within the sample. This information is lost upon closing. Subsequently, the compositional data no longer completely retains the information about the correlation of the elements in the original sample. That is, all the results obtained from the R-type statistical analysis method based on the related structure of compositional data represent only the characteristics of the components, excluding the characteristics of the elements of the sample (Zhou, 1997; Kork, 1977). Hence, the closure effect is not considered.

4.2. Identification of synthetical anomalies via factor analysis of multielement

4.2.1. Factor analysis of trace element

Factor analysis is among the commonly used methods for multivariate statistical analysis, which is often used to solve complex geological genesis and mineralization superposition problems; it also provides good decomposition to the superimposed geochemical field (Dong et al., 2008). By concentrating a large amount of geological data, a new dominant independent variable (factor) is extracted to reveal the interrelationship between variables, samples and material components, and geological processes. It provides a basis for studying the classification and causes of the variables.

In this paper, the R factor analysis based on principal component variables (KMO value is 0.709, Bartlett sphericity test is passed, and factor analysis hypothesis is met) was carried out by using the SPSS software. At an eigenvalue that is greater than 1 and accumulative variance contribution of 59.310%, 4 factors are extracted (Table 3), and the factor load matrix is rotated with maximum variance (Table 4). The factor scores of each sample are stored as variables in the sample attribute.

Table 4 indicates the following composition of each factor: the principal component of F1 is Ag, Cu, and Sn; F2 is Pb, Zn; F3 is Sb, Au, and As; and F4 is Mo. The variance contribution of factor F1 is 27.413%, which is the dominant factor in the study area. The main element is the medium–high temperature sulfurophilic element Ag–-Cu–Sn, which contains the main metallogenic elements, and the corresponding Ag and Cu may indicate the early sulfur phase (iron–copper sulfide phase) of the quartz–polymetallic sulfide stage, which reflects the main metallogenic process or stage. It can be used as a comprehensive indicator for the spatial accumulation of major metallogenic elements in the study area. The variance contribution of factor F2 is 12.253%. Pb and Zn may correspond to the late sulfide phase (lead–zinc sulfide phase), indicating the mineralization of Pb and Zn. The variance contribution of factor F3 is 10.357%, which is mainly composed of Sb–As cryogenic elements. Sb and As are the main elements of V and As

Table 2
Statistical characteristics of the elements in the borehole primary halo in Kekeshala deposit.

Element	Sample numbers	Minimum	Maximum	Mean	Standard deviation	Skewness	Kurtosis
As	4857	0.015	2025.000	14.06984	50.387050	18.257	592.929
Sb	4877	0.010	405.000	2.22656	8.635532	25.052	1020.501
Bi	4859	0.0070	951.0000	3.799353	33.6257382	17.806	384.090
Cu	4853	0.110	102,046.000	463.02930	3153.385790	14.527	315.648
Zn	4819	0.23	28,700.00	105.9122	612.26675	32.099	1235.970
W	4868	0.01	3051.00	12.1821	69.97708	23.070	820.873
Mo	4870	0.012	10,201.000	8.73180	159.967115	56.631	3472.557
Pb	4875	0.07	2000.00	23.0405	60.94074	20.592	569.656
Sn	4877	0.34	500.00	14.9948	68.14112	6.528	42.699
Ag	4872	0.030	100.000	0.93692	5.645653	9.749	112.488
Au	4867	0.042	1500.000	5.09901	40.079960	27.632	930.875

Note: in the element mass fraction, Au is 10^{-9} and the rest is 10^{-6}.

Table 3
Characteristic roots and total variance explained of R-factor analysis in Kekeshala deposit.

Factor	Initial eigenvalue			Load square sum			Rotating load square sum		
	Total	Variance (%)	Accumulate (%)	Total	Variance (%)	Accumulate (%)	Total	Variance (%)	Accumulate (%)
1	3.015	27.413	27.413	3.015	27.413	27.413	2.171	19.736	19.736
2	1.348	12.253	39.666	1.348	12.253	39.666	1.667	15.154	34.891
3	1.139	10.357	50.023	1.139	10.357	50.023	1.642	14.927	49.817
4	1.022	9.287	59.310	1.022	9.287	59.310	1.044	9.493	59.310
5	0.905	8.228	67.539						
6	0.859	7.809	75.348						
7	0.793	7.205	82.552						
8	0.692	6.287	88.840						
9	0.515	4.683	93.522						
10	0.450	4.091	97.613						
11	0.263	2.387	100.000						

Extraction method: principal component analysis.

Table 4
Orthometric rotating factor loading matrix for the R-factor analysis in the Kekeshala deposit[a].

Variable	Factor load			
	F1	F2	F3	F4
As	0.385	0.133	0.608	−0.010
Sb	−0.075	0.115	0.689	0.027
Bi	0.287	0.485	0.372	−0.012
Cu	0.815	0.101	0.126	0.026
Zn	0.006	0.763	0.032	−0.011
W	0.128	−0.058	0.450	0.433
Mo	−0.004	0.035	−0.087	0.921
Pb	0.089	0.845	0.080	0.025
Sn	0.722	−0.088	0.103	0.013
Ag	0.840	0.283	0.088	0.048
Au	0.142	0.045	0.638	−0.054

Extraction method: principal component analysis.
Rotation method: Kaiser standardized maximum variance method.
[a] The rotation has converged after five iterations.

as chalcophile elements, which belongs to semi-metallic amphoteric element at low temperature with similar geochemical behavior, strong migration ability, and are mostly distributed in the periphery of acid intrusive rock mass or near structure. The variance contribution of factor F4 is 9.287%, which is mainly a high-temperature element. It is easily enriched in the acid rock mass and can represent the element assemblage related to magmatic hydrothermal fluid.

4.2.2. Geochemical subdivision

According to the factor score of the sample, 4878 samples in the whole area are classified into four sample types. Each sample is assigned according to factor type corresponding to the highest score, and each category corresponds to a combination of a standard type element, representing a certain type of geochemical partition. In Surpac, according to the statistics of sample length with an average of approximately 5 m, the 3D block model of the mining area is established with grid dimensions of 10 m × 10 m × 5 m. Based on the sample points introduced after classification, the block model is spatially assigned by the nearest distance method. The 3D geochemical zoning map controlled by the borehole in the district can be obtained (Fig. 4).

The chemical zoning of F1 is mainly distributed near the Kekeshala L2 + 1 and L10 ore bodies in the middle and southern part of the study area, reflecting the main metallogenic location of Cu as revealed by the boreholes in the district, which agree with those of known orebodies. The chemical zoning of F2 is widely distributed, indicating the main location of the mineralization of Pb and Zn, and F3 as the type of the front halo element assemblage, and its chemical zoning is generally distributed in the head of the main orebody, which can be used as an indicator element in the deep metallogenic region. As the tail halo element assemblage, the chemical zoning of F4 generally reflects the end of a certain period of orebody mineralization, which is mainly in the acid intrusive rock or near the contact zone. It may also be related to its concealed bottom rock mass. In ore-prospecting, mineralization results from multistage synthesis and the occurrence of late denudation of the orebody. Hence, the primary halo of the orebodies at different metallogenic stages or the similar series bead orebody formed by the same metallogenic stage has complicated head-and-tail superposition structure.

4.3. Fractal analysis

4.3.1. Multifractal modeling of factor F1 through C–V multifractal method

The enrichment and loss processes of ore minerals and ore-forming elements in the metallogenic process are complex nonlinear process, especially when multiple stages are involved. Even the same metallogenic processes may undergo different metallogenic stages, making the main metallogenic elements inhomogeneous within the metallogenic domain. Multifractal model can be used to measure the dilution or enrichment degree and the spatial variability (Cheng, 2008). A previous factor analysis shows that factor F1 is the main metallogenic element assemblage, which reflects the main metallogenic process in the district. Its deep prospect can be used as a comprehensive indicator of the spatial aggregation of major metallogenic elements. In this paper, the factor F1 is selected to extract multielement synthetic deep prospect based on the C–V multifractal model.

In SPSS, the F1 score of 11 elements from 4878 samples in the study area can be saved as a result variable. To avoid the negative value of the late logarithm, it can be properly adjusted (minus the minimum value plus one) on the F1 variable. It will not change the curve form of the later scatter point fitting. The minimum value is −6.52333, making the adjustment value 7.52333. After dropping the sample containing the F1 factor variable (with attributes) in the Surpac, based on the known sample F1 factor score, the F1 factor block model is generated by the new F1 attribute of the 3D block model (previously established) and 3D interpolation. IDW is used as the interpolation method. Based on the distance between the exploration lines (40 m), the horizontal direction of the search radius is 80 m, the vertical direction is 40 m, the ratio of spindle to semi spindle is 0.5, the ratio of spindle to secondary axis is 1, the minimum number of samples to select is 3, whereas the maximum is 15. Based on the scoring frequency statistics of the F1 factor block model (completed in Surpac software, Fig. 5), the volume percentage of the different scores of the F1 factor can be counted. The scatter plot of concentration (F1 score) and cumulative volume (effective interpolation block percentage) can be drawn using the Excel software. The least

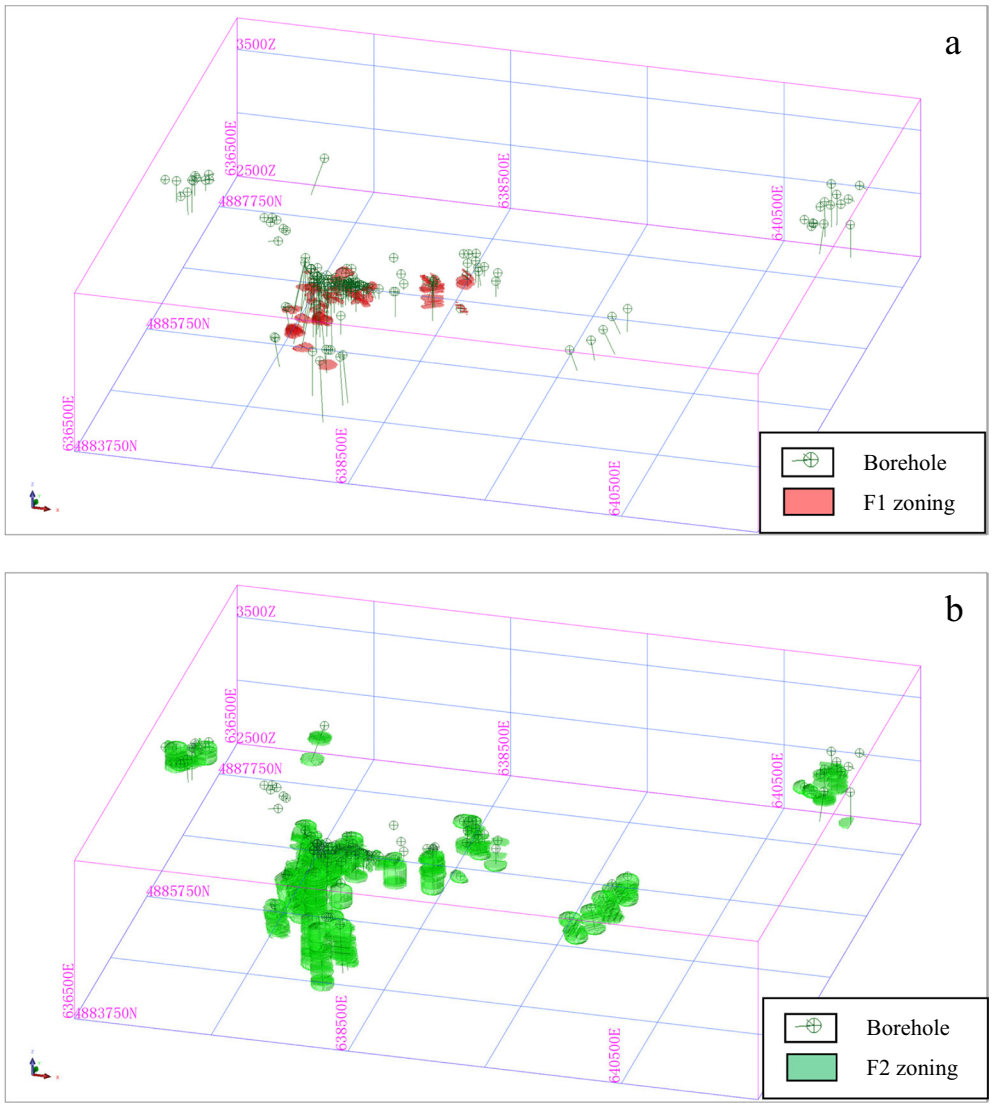

Fig. 4. 3D geochemical zoning map of the Kekeshala district.

squares method is used for fitting (Fig. 6), and the fractal dimension equation of F1 factor is obtained, which can be expressed as follows:

$$V(\rho) = 5.003\rho^{-3.069} \quad 0 < \rho < 9.82 \tag{2}$$

$$V(\rho) = 353.60\rho^{-354.3} \quad 9.82 \leq \rho < 9.85 \tag{3}$$

$$V(\rho) = 67.79\rho^{-66.97} \quad 9.85 \leq \rho < 9.98 \tag{4}$$

$$V(\rho) = 13.65\rho^{-12.78} \quad 9.98 \leq \rho \tag{5}$$

The C–V log–log plot shows that the F1 factor can be fitted using four straight lines, reflecting the existence of four scale-free regions in its spatial distribution. The slope of the low-value area is −3.069, and the goodness of fit R^2 is small, which is random and belongs to the barren host rocks. The main concentration (factor score) interval is above the second section, and the goodness of fit is above 0.8, which shows obvious correlation and good fitting degree, usually it is abnormal area. In this anomaly area, the slope of the second section is relatively large (the absolute value, the same below), which reflects the rapid decrease in frequency from low to high concentration, as well as the large area of distribution, which reflects the regional geological process that is closely related to mineralization. Moreover, the process rate in this area is possibly faster, and the boundary control is obvious, which belongs to the weakly deep prospect area. The third section has a relatively small straight slope, which reflects the relatively slow decrease in frequency of the high concentration and the smaller distribution area. It is mainly associated with the local mineralization process and the change in metallogenic conditions, which belongs to the moderately deep prospect area. The fourth section is relatively smaller compared with the previous sections, which reflects the slow decrease in concentration and the smallest distribution area, which is usually at the center of the moderately deep prospect that belongs to the highly deep prospect area.

4.3.2. *Predictive mapping of potential exploration targets*

The multifractal theory and model can depict the inhomogeneity and spatial variability of each metallogenic element in the metallogenic process. It can also divide the enrichment areas to guide the delineation of favorable metallogenic target areas. The spatial variation of ore-forming enrichment and dilution in the whole region can be determined using the multifractal dimension spectrum (Cheng, 2003, 2006). Fractal dimension exponent is an important parameter to quantify extremely complex fractal objects, such as non-smooth, irregular, and broken objects. Moreover, it is a measure of the complexity, roughness, irregularity, and the effective occupancy of space. A large fractal dimension exponent corresponds to a complex and rough fractal object; otherwise, the object is regular and smooth. According to the C–V multifractal

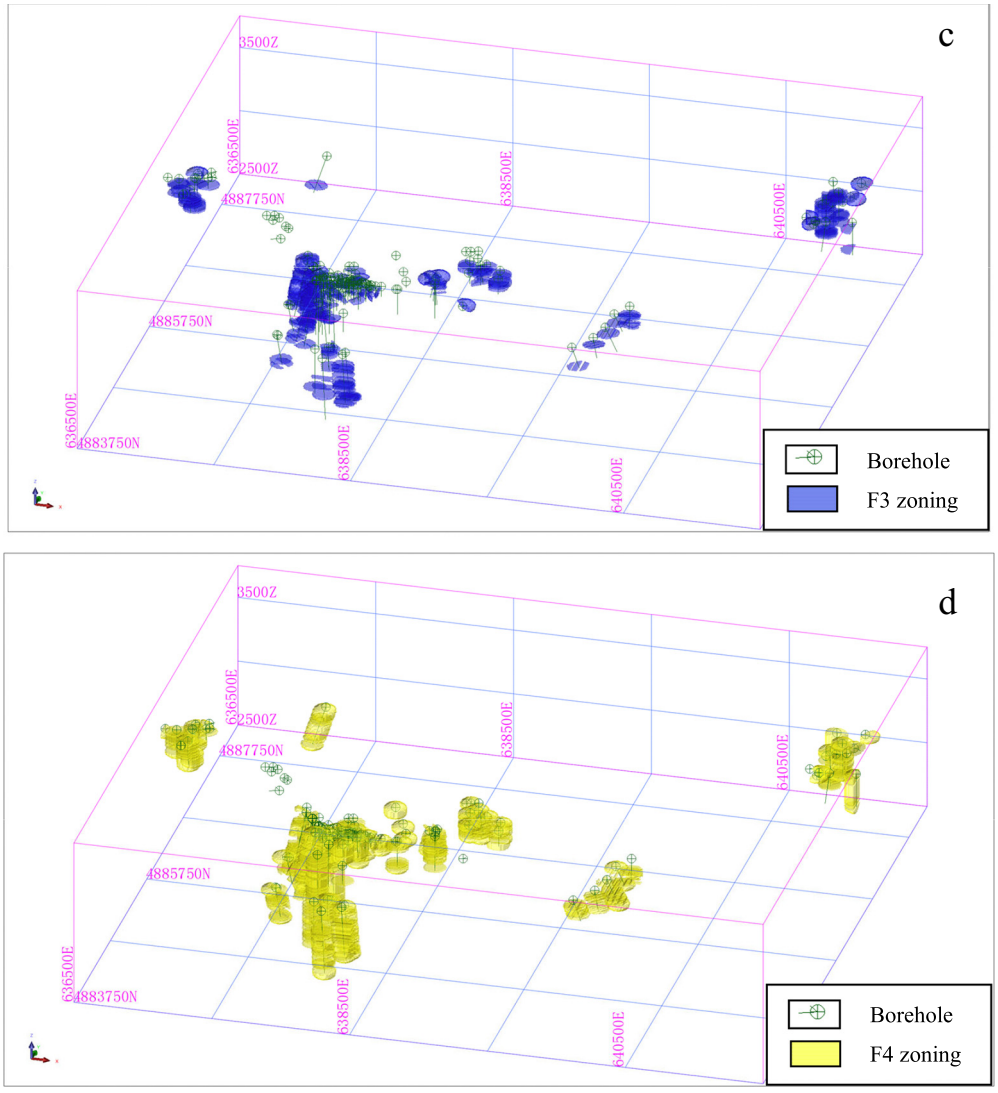

Fig. 4. (*continued*)

model in this district, the fractal characteristics of different fractal deep prospects can be calculated as shown in Table 5.

Table 5 shows that the fractal dimension exponent of factor F1 barren host rocks area is 3.069, indicating a uniform distribution in the 3D space. The weakly anomalous fractal dimension exponent is 354.30, which shows the irregularity and complexity of its spatial coverage and geometry. This value may be related to the complex water-rock interaction in the carbonate rocks of the Hudukedaban formation (O_3h)

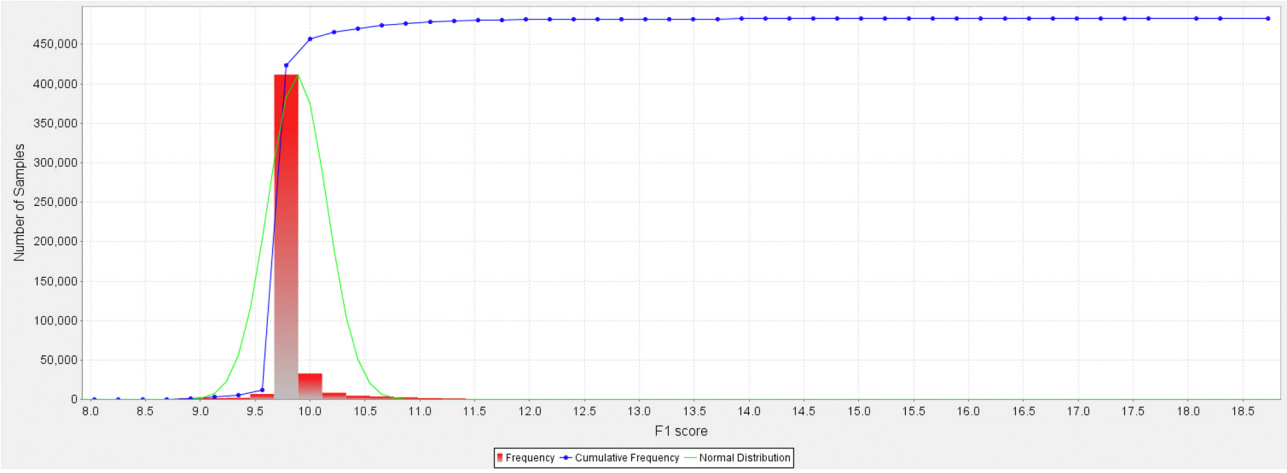

Fig. 5. Histogram of the scoring frequency statistics for the F1 factor block model.

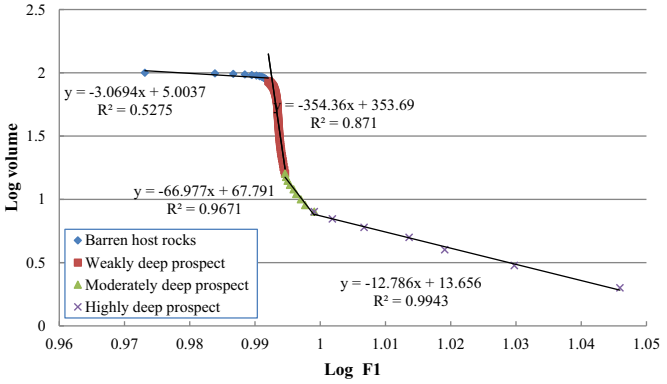

Fig. 6. Log–log plot of the cumulative volume versus F1 factor score in the Kekeshala district.

Table 5
Statistical characteristics of different fractal deep prospects.

Deep prospect classification based on C–V model	Fractal dimension exponent	Statistical fitting degree (R^2)	Fractal inflection point (F1-adjusted score)
Barren host rocks	3.069	0.527	0
Weak	354.30	0.871	9.82
Moderate	66.97	0.967	9.85
High	12.78	0.994	9.98

intruded by the Huster granite (~368 Ma), which may reflect a contact zone structure and a favorable metallogenic geological environment for skarn deposits. The fractal dimension exponent at the moderately deep prospect is 66.97, which follows a strong agglomeration law. However, the exponent decreases obviously, reflecting the superposition of complex mineralization in the favorable metallogenic geological environment, forming the local enrichment of the corresponding elements, which has great potential for prospecting. Mineralization is usually inherited. The Re–Os age of molybdenum (~295 Ma) in the deposit may represent the superposition of another magmatic hydrothermal metallogenic event in the early Permian period. This type of mineralization at different geological periods superimpose each other in space, which mostly occur in areas with strong tectonic and magmatic activity and had relatively small coverage, making the fractal dimension exponent relatively low. The fractal dimension exponent at the highly deep prospect is 12.78, which is reclustered in the moderately deep prospect. This finding reflects the concentration center of moderately deep prospect and that its prospecting potential is the greatest. Based on the statistical anomalous inflection point, the moderately and highly deep prospect of the factor F1 can be extracted as the prospecting target (Fig. 7).

The known orebodies delineated by boreholes are superimposed on some moderately and highly deep prospects (Fig. 8), showing a good correlation between them. The moderately deep prospect is mainly distributed within and around L2 + 1 and L10 orebodies, which accurately reflects the spatial distribution and trend of orebodies, especially for L2 + 1. Good moderately and highly deep prospects are present along the deep contact zone. This finding indicates that a large extension of prospecting space remains in the deep part of the L2 + 1.

5. Conclusions

The Kekeshala deposit is a typical skarn-copper deposit. The orebody is controlled by the contact zone between the Huster rock mass and the carbonatite strata (O_3h). The orebody shape is complex, and the trend of deep extension is unknown. In this paper, 3D visualization, factor analysis, and C–V multifractal model are combined to study the geochemical samples of primary halo in Kekeshala district. Taking the F1 factor as the fractal object, which reflects the main metallogenic geological process of the deposit, the weakly, moderately, and highly deep prospect are extracted through C–V fractal modeling. It provides a basis for the screening of target regions. The results of this study can be summarized as follows:

(1) Based on the Surpac software, 167 boreholes in the Kekeshala mining area are modeled and visualized, from which 4878 3D borehole primary halo samples are extracted, and a 3D block model of the borehole primary halo is established. Subsequently, a basic model was created for succeeding analysis and visualization.
(2) The Kekeshala deposit is mainly a skarn-copper deposit. Factor analysis of the geochemical data of the borehole primary halo shows that the factor F1 consists of the combination of the main metallogenic elements Cu and Ag in the study area, F2 reflects Pb–Zn mineralization, F3 reflects As–Sb front halo association, and F4 reflects subore halo association. F1 may reflect the early sulfide phase of the quartz-polymetallic sulfide stage (iron–copper sulfide phase), which represents the main metallogenic process or stage. It

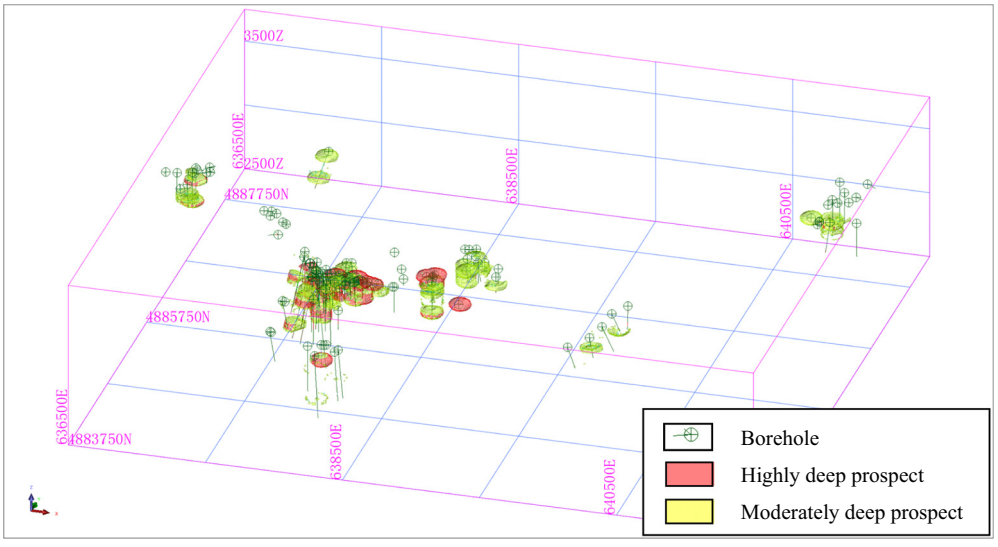

Fig. 7. Moderately and highly deep prospect of the factor F1 in the Kekeshala district.

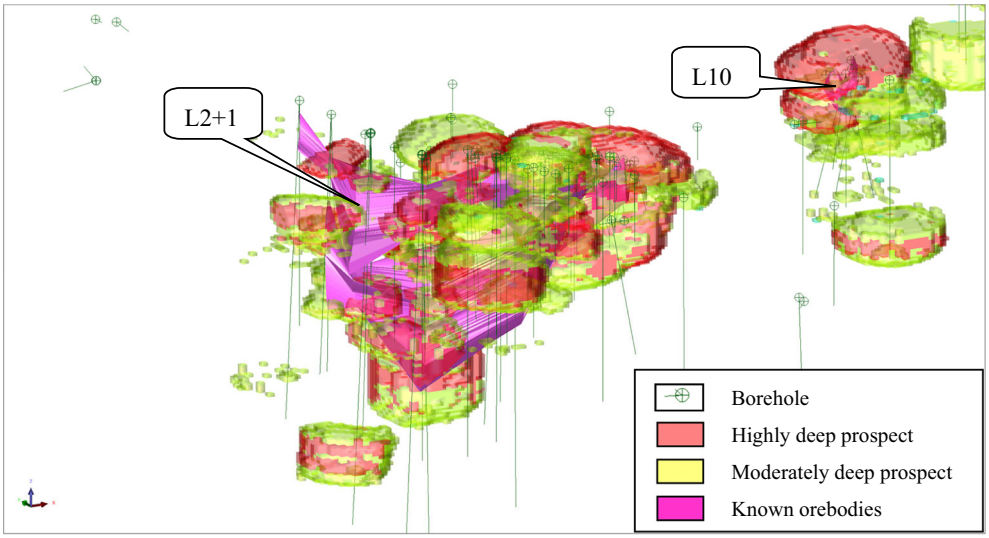

Fig. 8. Deep prospects and the known orebodies superposition.

can be used as a comprehensive indicator of the spatial aggregation of major metallogenic elements in the study area. The chemical zoning of F1 is in good agreement with those of known main orebodies.

(3) The C–A fractal model of factor F1 shows that the fractal fitting line of the study area consists of four segments, reflecting the multifractal characteristics. The inflection point indicates that the geochemical barren host rocks area and the weakly, moderately, and highly deep prospect can be divided. The weakly deep prospect reflects the contact zone structure between the Huster rock mass and the carbonatite strata (O_3h). The moderately deep prospect may reflect the complex mineralization process based on the ore-bearing strata and favorable tectonic conditions. The highly deep prospect reflects the center of the moderately deep prospect.

(4) Based on the fractal deep prospect analysis of factor F1, the moderately and highly deep prospect can well reflect the favorable metallogenic geological conditions and can be used as the basis for delineating the prospecting target. The known main orebodies L2 + 1 and L10 are in good agreement with some moderately and highly deep prospects. The fractal deep prospect of geochemical factor F1 has potential application in ore-prospecting and prediction, and can thus be effectively used to explore the depth and edge of known deposits.

Acknowledgements

This work was supported by the National Natural Science Foundation of China (No. 41572062), National Key R & D Program (No. 2018YFC0604003), and the Comprehensive research project on the return of two rights funds by the Central Committee (No. Y15-1-LQ04). The authors would like to thank the Seventh Geological Group of Xinjiang Geology and Mining Bureau of China for their logistic support and authorization to access the Kekeshala drillcores and dataset. The authors acknowledge the editor and reviewers of this paper for their comments and valuable remarks.

References

Afzal, P., Khakzad, A., Moarefvand, P., Rashidnejad, O.N., Esfandiari, B., Fadakar, A.Y., 2010. Geochemical anomaly separation by multifractal modeling in Kahang (Gor) porphyry system, Central Iran. J. Geochem. Explor. 104, 34–46.

Afzal, P., Fadakar, A.Y., Khakzad, A., Moarefvand, P., Rashidnejad, O.N., 2011. Delineation of mineralization zones in porphyry Cu deposits by fractal concentration–volume modeling. J. Geochem. Explor. 18, 220–232.

Afzal, P., Fadakar Alghalandis, A., Moarefvand, P., Rashidnejad Omran, N., Asadi Haroni, H., 2012. Application of power-spectrum–volume fractal method for detecting hypogene, supergene enrichment, leached and barren zones in Kahang Cu porphyry deposit, Central Iran. J. Geochem. Explor. 112, 131–138.

Afzal, P., Madani, N., Shahbeik, Sh., Yasrebi, A.B., 2015. Multi-Gaussian kriging: a practice to enhance delineation of mineralized zones by concentration–volume fractal model in Dardevey iron ore deposit, SE Iran. J. Geochem. Explor. 158, 10–21.

Afzal, P., Eskandarnejad Tehrani, M., Ghaderi, M., Hosseini, M.R., 2016. Delineation of supergene enrichment, hypogene and oxidation zones utilizing staged factor analysis and fractal modeling in Takht-e-Gonbad porphyry deposit, SE Iran. J. Geochem. Explor. 161, 119–127.

Agnew, P., 2004. Applications of geochemistry in targeting with emphasis on large stream and lake sediment data complications. In: SEG Conference, Sydney, 2004.

Agterberg, F.P., 1995. Multifractal modeling of the sizes and grades of giant and supergiant deposits. Int. Geol. Rev. 37, 1–8.

Agterberg, F.P., 2012. Multifractals and geostatistics. J. Geochem. Explor. 122, 113–122.

Agterberg, F.P., Cheng, Q., Wright, D.F., 1993. Fractal modeling of mineral deposits. In: Elbrond, J., Tang, X. (Eds.), 24th APCOM Symposium Proceeding, Montreal, Canada, pp. 43–53.

Aitchison, J., 1984. The statistical analysis of geochemical compositions. J. Int. Assoc. Math. Geol. 16 (6), 531–564.

Bansal, A.R., Gabriel, G., Dimri, V.P., Krawczyk, C.M., 2011. Estimation of the depth to the bottom of magnetic sources by a modified centroid method for fractal distribution of sources: an application to aeromagnetic data in Germany. Geophysics 76, L11–L22.

Carlson, C.A., 1991. Spatial distribution of ore deposits. Geology 19, 111–114.

Carranza, E.J.M., 2008. Geochemical anomaly and mineral prospectivity mapping in GIS. In: Handbook of Exploration and Environmental Geochemistry. vol. 11 Elsevier, Amsterdam (351 pp.).

Carranza, E.J.M., Sadeghi, M., 2012. Primary geochemical characteristics of mineral deposits–implications for exploration. Ore Geol. Rev. 45 (1–4).

Carranza, E.J.M., Owusu, E.A., Hale, M., 2009. Mapping of prospectivity and estimation of number of undiscovered prospects for lode gold, southwestern Ashanti Belt, Ghana. Mineral. Deposita 44, 915–938.

Cheng, Q., 1995. The perimeter–area fractal model and its application to geology. Math. Geol. 27, 69–82.

Cheng, Q., 2003. Fractal and multifractal modeling of hydrothermal mineral deposit spectrum: application to gold deposits in Abitibi Area, Ontario, Canada. J. China Univ. Geosci. (03), 11–18.

Cheng, Q., 2004. A new model for quantifying anisotropic scale invariance and for decomposition of mixing patterns. Math. Geol. 36, 345–360.

Cheng, Q., 2006. Singularity-generalized self-similarity-fractal spectrum (3S) models. Earth Sci. J. China Univ. Geosci. 31 (03), 337–348.

Cheng, Q., 2007. Mapping singularities with stream sediment geochemical data for prediction of undiscovered mineral deposits in Gejiu, Yunnan Province, China. Ore Geol. Rev. 32, 314–324.

Cheng, Q., 2008. Singularity of mineralization and multifractal distribution of mineral deposits. Petrol. Geochem. 27 (03), 298–305.

Cheng, Q., 2011. Singularity modeling of geo-anomalies and recognition of anomalies caused by buried sources. Earth Sci. 36 (02), 307–316.

Cheng, Q., 2012. Singularity theory and methods for mapping geochemical anomalies caused by buried sources and for predicting undiscovered mineral deposits in covered areas. J. Geochem. Explor. 122, 55–70.

Cheng, Q., Agterberg, F.P., Ballantyne, S.B., 1994. The separation of geochemical anomalies from background by fractal methods. J. Geochem. Explor. 54, 109–130.

Davis, J.C., 1973. Statistical Data Analysis in Geology. John Wiley & Sons.

Dong, Q., Chen, J., Tang, Y., 2008. Application of R type factor analyses in mineralization prognosis by an example of Huangbuling gold deposit, Shandong Province. Geol. Prospect. 44 (4), 64–68.

Ebadi Rajoli, M., Afzal, P., Moarefvand, P., 2015. Classification of mineralized veins using concentration volume (C-V) fractal modeling: a case study from Chah-Mesi Cu-Au vein deposit, SE Iran. Arab. J. Geosci. 8 (10), 8249–8262.
Egozcue, J.J., Pawlowsky-Glahn, V., Mateu-Figueras, G., Barceló-Vidal, C., 2003. Isometric log ratio transformations for compositional data analysis. Math. Geol. 35 (3), 279–300.
Filzmoser, P., Hron, K., Reimann, C., 2009. Principal component analysis for compositional data with outliers. Environmetrics 20 (6), 621–632.
Goncalves, M.A., Mateus, A., Oliveira, V., 2001. Geochemical anomaly separation by multifractal modeling. J. Geochem. Explor. 72, 91–114.
Gu, X., Zhang, Y., Wang, X., Zhang, L., Dong, L., Tu, Q., Liu, R., Gao, H., 2013. Geochronology of intrusive rocks and associated ores of the Kekesala-Ai-musidaiyi Fe-Cu deposit in the West Tianshan, Xinjiang and its geologic significance. Earth Sci. Front. 20 (6), 195–209.
Hashemi Marand, Gh., Jafari, M.R., Afzal, P., Khakzad, A., 2018. Determination of relationship between silver and lead mineralization based on fractal modeling in Mehdiabad Zn-Pb-Ag deposit, Central Iran. Geosciences 106, 111–118.
Kork, J.O., 1977. Examination of the Chayes-Kruskal procedure for testing correlations between proportions. Math. Geol. 9 (6), 543–562.
Li, C., Ma, T., Shi, J., 2003. Application of a fractal method relating concentrations and distances for separation of geochemical anomalies from background. J. Geochem. Explor. 77, 167–175.
Liu, H., Huang, H., Li, G., Xue, W., Zhang, Z., Liu, B., Ma, D., Dong, L., 2015. Factor analysis in geochemical survey of the Shangxu gold deposit, Northern Tibet. Geol. China 42 (04), 1126–1136.
Mandelbrot, B., 1983. The Fractal Geometry of Nature, Updated and Augmented edition. W.H. Freeman and Company, New York (468 pp.).
Raines, G.L., 2008. Are fractal dimensions of the spatial distribution of mineral deposits meaningful? Nat. Resour. Res. 17, 87–97.
Sadeghi, B., Moarefvand, P., Afzal, P., Yasrebi, A.B., Daneshvar Saein, L., 2012. Application of fractal models to outline mineralized zones in the Zaghia iron ore deposit, Central Iran. J. Geochem. Explor. 122, 9–19.
Shi, Y., Ji, H., Lu, J., Ma, L., Duan, G., 2004. Factor analysis method and application of stream sediment geochemical partition. Geol. Prospect. 05, 73–76.
Sim, B.L., Agterberg, F.P., Beaudry, C., 1999. Determining the cutoff between background and relative base metal contamination levels using multifractal methods. Comput. Geosci. 25, 1023–1041.
Turcotte, D.L., 1986. A fractal approach to the relationship between ore grade and tonnage. Econ. Geol. 18, 1525–1532.
Turcotte, D.L., 1997. Fractals and Chaos in Geology and Geophysics, 2nd edn. Cambridge University Press, Cambridge, United Kingdom (398 pp.).
Wang, Q.F., Deng, J., Liu, H., Wang, Y., Sun, X., Wan, L., 2011. Fractal models for estimating local reserves with different mineralization qualities and spatial variations. J. Geochem. Explor. 108, 196–208.
Wang, G., Zhang, S., Yan, C., Song, Y., Sun, Y., Li, D., Xu, F., 2011a. Mineral potential targeting and resource assessment based on 3D geological modeling in Luanchuan region, China. Comput. Geosci. 37, 1976–1988.
Wang, G., Zhang, S., Yan, C., Xu, G., Ma, M., Li, K., Feng, Y., 2011b. Application of the multifractal singular value decomposition for delineating geophysical anomalies associated with molybdenum occurrences in the Luanchuan ore field (China). J. Appl. Geophys. 86, 109–119.
Wang, G., Carranza, E.J.M., Zuo, R., Hao, Y., Du, Y., Pang, Z., Sun, Y., Qu, J., 2012. Mapping of district-scale potential targets using fractal models. J. Geochem. Explor. 122, 34–46.
Zhang, B., 1989. Theory and Method of Ore-belt Geochemical Research. Geological Publishing House, Beijing.
Zhang, Y., Zhou, Y., 2012. Application of singularity theory in prediction of silver and gold mineral deposits in Qinzhou-Hangzhou tectonic joint belt Pangxidong Area, Guangdong, China. J. Cent. S. Univ. (Sci. Technol.) 43 (9), 3558–3564.
Zhao, P., Chi, S., 1991. A preliminary view on geological anomaly. Earth Sci. 03, 241–248.
Zhao, S., Wei, J., Gao, X., et al., 2012. Factor analysis in the geochemical subdivisions: taking 1:50 000 debris geochemical survey in the Shibanjing area of Inner Mongolia as an example. Geol. Sci. Technol. Inf. 31 (02), 27–−34.
Zhou, D., 1997. Effect of logratio transformation on classifying compositions. In: Pawlowsky (Ed.), Proceedings of IAMG' 97, Part 1. CIMNE, Barcelona, pp. 102–−105.
Zuo, R., 2011a. Decomposing of mixed pattern of arsenic using fractal model in Gangdese belt, Tibet, China. Appl. Geochem. 26 (Suppl), S271–S273.
Zuo, R., 2011b. Identifying geochemical anomalies associated with Cu and Pb–Zn skarn mineralization using principal component analysis and spectrum–area fractal modeling in the Gangdese Belt, Tibet (China). J. Geochem. Explor. 111 (1–2), 13–22.
Zuo, R., 2012. Exploring the effects of cell size in geochemical mapping. J. Geochem. Explor. 112, 357–367.
Zuo, R., Agterberg, F.P., Cheng, Q., Yao, L., 2009a. Fractal characterization of the spatial distribution of geological point processes. Int. J. Appl. Earth Obs. Geoinf. 11, 394–402.
Zuo, R., Cheng, Q., Xia, Q., 2009b. Evaluation of the uncertainty in estimation of metal resources of skarn tin in Southern China. Ore Geol. Rev. 35, 415–422.
Zuo, R., Cheng, Q., Xia, Q., 2009c. Application of fractal models to characterization of vertical distribution of geochemical element concentration. J. Geochem. Explor. 102, 37–43.
Zuo, R., Cheng, Q., Xia, Q., Agterberg, F.P., 2009d. Application of fractal models to distinguishing between different mineral phases. Math. Geosci. 41, 71–80.
Zuo, R., Xia, Q., Zhang, D., 2013. A comparison study of the C–A and S–A models with singularity analysis to identify geochemical anomalies in covered areas. Appl. Geochem. 33, 165–172.
Zuo, R., Wang, J., Chen, G., Yang, M., 2015. Identification of weak anomalies: a multifractal perspective. J. Geochem. Explor. 154, 200–212.